

Similarity theory of lubricated Hertzian contacts

J. H. Snoeijer,¹ J. Eggers,² and C. H. Venner³

¹*Physics of Fluids and J.M. Burgers Center for Fluid Dynamics, University of Twente, P.O. Box 217, 7500 AE Enschede, The Netherlands*

²*Department of Mathematics, University of Bristol, University Walk, Bristol BS8 1TW, United Kingdom*

³*Faculty of Engineering Technology, Engineering Fluid Dynamics, University of Twente, P.O. Box 217, 7500 AE Enschede, The Netherlands*

(Received 16 May 2013; accepted 14 October 2013; published online 28 October 2013)

We consider a heavily loaded, lubricated contact between two elastic bodies at relative speed U , such that there is substantial elastic deformation. As a result of the interplay between hydrodynamics and non-local elasticity, a fluid film develops between the two solids, whose thickness scales as $U^{3/5}$. The film profile h is selected by a universal similarity solution along the upstream inlet. Another similarity solution is valid at the outlet, which exhibits a local minimum in the film thickness. The two solutions are connected by a hyperbolic problem underneath the contact. Our asymptotic results for a soft sphere pressed against a hard wall are shown to agree with both experiment and numerical simulations. © 2013 AIP Publishing LLC. [<http://dx.doi.org/10.1063/1.4826981>]

The lubricating flow between two moving solids serves to prevent wear, as well as to reduce friction.¹ In many important applications, and in particular for soft materials (rubbers, gels, or tissue), the solid is deformed significantly with respect to the thickness of the lubrication layer, and hydrodynamic and elastic effects become coupled.^{2–4} The resulting elasto-hydrodynamic equations are non-local, so that progress on this problem has so far been limited mostly to numerical studies.^{1,5,6}

In the limiting case of small elastic deformations, the problem can be solved perturbatively and reduces to a set of ordinary differential equations.^{2,3,7} For the opposite case of strong deformations, the contact area becomes flat as in a classical Hertzian contact,⁸ except for the effect of the thin lubrication layer.^{9–11} Here we show that at the edge of the contact area, the film thickness is described by a similarity solution, whose shape is governed by an integro-differential equation, as opposed to the ordinary differential equations encountered in most singular fluid problems.¹² By solving the non-local similarity equation, we treat the selection problem for the film thickness, which turns out to be a non-local version of Bretherton's problem¹³ for the motion of a bubble in a tube. Our analysis is reminiscent of that by Bissett¹⁰ for a two-dimensional line contact, who also formulated the problem in terms of a local equation near the edge of the contact. However, we show that the present formulation in terms of similarity solution allows for a detailed description of three-dimensional contacts. In addition, we validate all results by numerical simulation of two- and three-dimensional lubricated contacts, revealing the universality of the gap shape and the pressure profile, as well as the scaling with load for the first time.

The viscous fluid flow in the narrow gap between the solids is well described by Reynolds' lubrication theory,¹⁴ while the elastic part follows from the deformation of an elastic half-space in response to a pressure distribution over the surface.⁸ The resulting coupled elasto-hydrodynamic equations have been used for a long time to describe highly deformed contacts,^{1,5,6,10,15,16} the collision of spheres,¹⁷ and small deformations in the lubrication regime.^{2,3}

We first treat the two-dimensional problem of an elastic cylinder moving parallel to a non-deformable wall, see Fig. 1. The generalization to two different elastic media and to other shapes, including three-dimensional ones, is straightforward and will be outlined below. We consider a reference system in which the cylinder is stationary, and the substrate moves at speed U to the right,

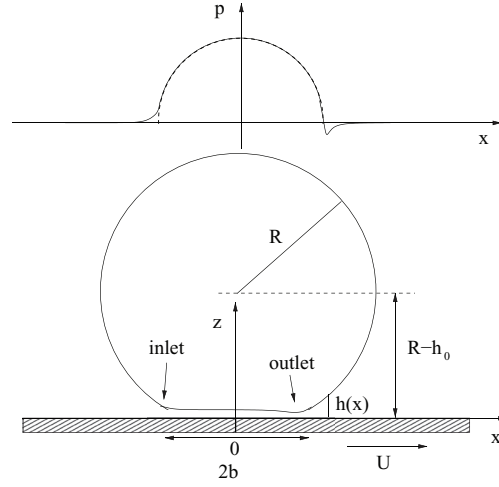


FIG. 1. Sketch of an elastic cylinder with the solid moving to the right, equivalent to a cylinder moving to the left; at the top, the pressure distribution in the gap.

so that the gap width is described by a function $h(x)$. Assuming that the pressure is constant over the gap width, Stokes' equation $\nabla p = \eta \Delta \mathbf{u}$ as well as the no-slip boundary conditions at both solids are satisfied by the horizontal velocity component

$$u = U \left(1 - \frac{z}{h} \right) + \frac{p_x}{2\eta} (z^2 - zh), \quad (1)$$

where η is the fluid viscosity and p_x the pressure gradient in the horizontal direction. Integrating (1) over the gap, one obtains the volume flux Q , which must be independent of x for an incompressible fluid. Putting $h^* = 2Q/U$, we obtain the lubrication equation

$$p_x = 6U\eta \frac{h - h^*}{h^3}. \quad (2)$$

We remark that for fore-aft symmetric bodies, p as computed from (2) is antisymmetric with respect to the line of symmetry, so that the *load*

$$L = \int_{-\infty}^{\infty} p dx \quad (3)$$

vanishes exactly. For the lubricated contact to support any load this symmetry must be broken; this may be due to cavitation¹⁸ or, when the pressures are sufficiently large, by elastic deformation.

In Ref. 3, L is calculated perturbatively in the limit of vanishing load; like in Ref. 10 we now treat the opposite limit of large loads, that lead to deformations that are large with respect to the gap thickness but still small enough to be described by linear elasticity. For any value of L , the gap width is then described by

$$h(x) = c + \frac{x^2}{2R} - \frac{2(1 - \sigma^2)}{\pi E} \int_{-\infty}^{\infty} p(x') \ln |x - x'| dx', \quad (4)$$

where σ is Poisson's ratio and E Young's modulus. If the rigid wall is replaced by another elastic medium with Poisson's ratio σ' and Young's modulus E' , the combination $(1 - \sigma^2)/E$ is to be replaced by the effective value $(1 - \sigma^2)/E + (1 - \sigma'^2)/E'$ throughout.⁸ The first parabolic part of (4) represents the undeformed cylinder (and c is a constant to be determined), while the second part accounts for the elastic deformation.^{3,8} As is classical in this context, this elastic deformation is solved by a Green's function approach, where the kernel is the response to a localized force on a two-dimensional medium. The mathematical problem consists in solving the coupled systems (2) and (4)—the challenge lies in treating the nonlocal coupling introduced by (4).

To begin, we recall the classical Hertz problem of a dry contact between an elastic cylinder and a rigid wall. It will serve as the “outer” solution to our problem, valid outside an asymptotically small region at the edge of the dry contact. For the dry contact, we must solve (4) alone, subject to the condition that h be zero inside the contact region $|z| \leq b$, and $p = 0$ for $|z| > b$. The result is that the maximum pressure, the width of the contact, and the maximum deformation, respectively, are¹⁹

$$p_m = \frac{2L}{\pi b}; \quad b = \left(\frac{4LR(1 - \sigma^2)}{\pi E} \right)^{1/2}; \quad h_0 = \frac{b^2}{2R}. \quad (5)$$

From now on we will normalize x using b , the gap thickness h by $2h_0$, and p by p_m , while keeping the same notation as before. Then the exact solution of the Hertz problem is¹⁹

$$\bar{p} = \sqrt{1 - x^2} \Theta(1 - x^2), \quad (6)$$

$$\bar{h} = \left(|x| \sqrt{x^2 - 1} - \ln |x + \sqrt{x^2 - 1}| \right) \frac{\Theta(x^2 - 1)}{2}, \quad (7)$$

where Θ is the Heaviside step function. Formally, this is the solution to our problem for zero speed; the semicircular pressure distribution (6) is shown as the dashed line at the top of Fig. 1.

Rewriting the lubrication equation using the scales (5) and (2) becomes

$$p_x = \lambda \frac{h - h^*}{h^3}, \quad (8)$$

where

$$\lambda = \frac{3\pi^2}{4} \frac{\eta U R E}{L^2(1 - \sigma^2)} \quad (9)$$

is the sole dimensionless parameter of the problem. We are interested in the limit of small λ (i.e., large loads), while previous work^{2,3} studied the same equations for large λ .

Note that \bar{p}_x becomes infinite at the edge of the contact zone, where we have to introduce a thin boundary layer to regularize the problem. To localize the elastic problem in that region, we take the second derivative of (4) and integrate by parts once, to find in dimensionless variables:

$$h''(x) = 1 - \frac{1}{\pi} \int_{-\infty}^{\infty} \frac{p'(x')}{x - x'} dx' \equiv 1 - \mathcal{H}(p')(x), \quad (10)$$

where $\mathcal{H}(f)$ denotes the Hilbert transform of f .²⁰ We are looking for similarity solutions to (8) and (10) of the form¹²

$$h = \lambda^{\alpha_1} H_{\pm} \left(\frac{x \pm 1}{\lambda^{\beta}} \right), \quad p = \lambda^{\alpha_2} P_{\pm} \left(\frac{x \pm 1}{\lambda^{\beta}} \right), \quad (11)$$

where the $+$ sign refers to the inlet, the $-$ sign to the outlet. Inserting (11) into (8) and (10), one finds that $\alpha_1 = (2\beta + 1)/3$ and $\alpha_2 = (1 - \beta)/3$. To find β , note that the similarity profiles have to match onto the Hertz solution (6), which behaves like $\bar{p} \approx \sqrt{2(1 \pm x)}$ at the inlet and outlet, respectively. In terms of the similarity variable $\xi = (x \pm 1)/\lambda^{\beta}$, this means that $p \approx \lambda^{\beta/2} \sqrt{\pm 2\xi}$, and hence $P_{\pm}(\xi) \approx \lambda^{\beta/2 - \alpha_2} \sqrt{\pm 2\xi}$ for $\xi \rightarrow \pm\infty$. But since the inner solution P should no longer depend on λ , this means that $\alpha_2 = \beta/2$, and so $\alpha_1 = 3/5$, $\alpha_2 = 1/5$, and $\beta = 2/5$. These scalings have been suggested before on the basis of numerical simulations,²¹ scaling,⁹ and asymptotic analysis.^{10,11} Note that in the limit $\lambda \rightarrow 0$ the profile is asymptotically flat: the characteristic scale for the gap height $h \sim \lambda^{3/5}$ is much smaller than the scale for $x \sim \lambda^{2/5}$, ensuring that lubrication theory applies.

Using the scalings given above, (8) and (10) turn into the similarity equations

$$P' = \frac{H - H^*}{H^3}, \quad H''(\xi) = -\mathcal{H}(P')(\xi), \quad (12)$$

since the constant in (10) is subdominant. The difference between the inlet and outlet solutions is that the boundary conditions for $\xi \rightarrow \pm\infty$ are flipped; the conditions for P_{\pm} given above result in $H \approx H^* \pm H^{*3}/\sqrt{\pm 2\xi}$ for $\xi \rightarrow \pm\infty$, while on the other side $H_{\pm} \approx 2\sqrt{2}(\mp\xi)^{3/2}/3$ for $\xi \rightarrow \mp\infty$. The local system of Eq. (12) is essentially equivalent to that found by Ref. 10.

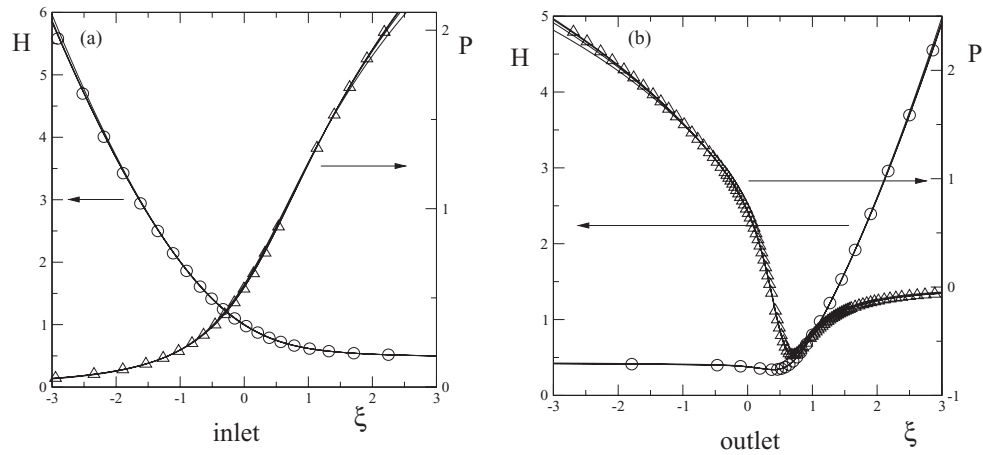


FIG. 2. Similarity profiles for the gap thickness $H(\xi)$ (circles) and the pressure $P(\xi)$ (triangles), as obtained for the inlet (a) and for the outlet (b). The symbols are obtained from the similarity theory (12), while the solid lines are rescaled profiles of the full numerical solution with $\lambda = 10^{-3}$, $\lambda = 10^{-4}$, $\lambda = 10^{-5}$, and $\lambda = 10^{-6}$.

We solved (12) numerically, both for the inlet and the outlet, using a generalized Newton–Raphson method,²² with the boundary conditions given above. The results are shown in Fig. 2 (symbols). We find that the inlet solution selects a unique value of $H^* = 0.4467\dots$, so that the (*dimensional*) gap thickness under the cylinder becomes

$$h_{gap} = H^* \left(\frac{\pi(3\eta UR)^3(1 - \sigma^2)^2}{2LE^2} \right)^{1/5}. \quad (13)$$

Since there is only a single free constant h^* in (8), the asymptotic film thickness of the outlet solution must be the same: we can use the universal constant H^* selected at the inlet to calculate the outlet solution. This mechanism is similar to the selection of the fluid film thickness around a large bubble rising in a tube, known as the Bretherton problem,¹³ or of the film below a flexible scraper.²³ Interestingly, the profile at the front of the Bretherton bubble is monotonic (like the similarity profile at the inlet, cf. Fig. 2, top), but exhibits a local minimum at the rear, corresponding to the outlet profile, Fig. 2, bottom. The pressure profile at the outlet becomes negative for positive ξ , corresponding to a small negative pressure region of size $\lambda^{2/5}$, as sketched at the top of Fig. 1. Except for these boundary regions at the edge of the contact, the pressure distribution has become symmetric, a complete reversal from the antisymmetric distribution found for the lubrication problem of an undeformed cylinder.

We have checked the validity of our asymptotic approach by comparing to a series of numerical simulations of (2) and (4) for increasingly small λ . Equations (2) and (4) and their three-dimensional equivalents were solved using multigrid/multilevel techniques,^{6,24} the efficiency of which allows to solve 2D as well as 3D problems for small gap sizes at high accuracy. Profiles at the inlet and outlet have been rescaled according to (11), and results are shown as the solid lines in Fig. 2. A small deviation is visible for the largest λ , but then almost perfect agreement is found; note that there is no adjustable parameter apart from a shift in ξ , which is arbitrary.

The qualitative shape of the gap profile, with a minimum at the outlet has already been reported experimentally in, e.g., Refs. 25 and 26. More recently, measurements of the gap thickness between a rubber ball and a plate moving at speed U have been reported for speeds varying over one-and-a-half decades.²⁷ The gap thickness h_{gap} at the center of the sphere was found to scale with an exponent $\alpha_1 = 0.57 \pm 0.05$ (reported as $\alpha_1 = 0.6$ in Ref. 28), in good agreement with^{9,10} and the current analysis. This, however, is in significant disagreement with the scaling argument by Refs. 27–30, predicting $\alpha_1 = 1/2$. The reason is that it is based on the erroneous assumption that viscous effects act over the entire region of the Hertzian contact. Our similarity theory shows that this is not the case, since viscosity acts only in the boundary layer near the inlet/outlet of the contact.

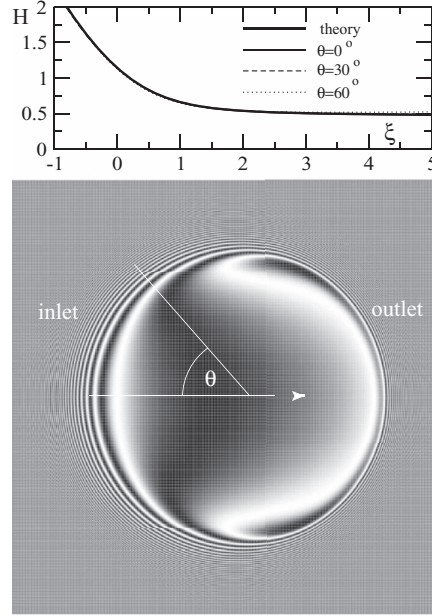


FIG. 3. (Top) Comparison between the present theory and numerical simulations of inlet profiles underneath an elastic sphere ($\lambda/\cos\theta = 0.62 \times 10^{-4}$, at angles of 0° , 30° , and 60°) relative to the direction of motion (left edge in the bottom figure). (Bottom) Simulation of the fluid film underneath a sphere pressed into a solid wall, thickness indicated by interference fringes; the solid wall is moving to the right.

Now we come to the physically most relevant case of a three-dimensional elastic body which is not cylindrical, for which an exact Hertz solution is in general not available. However, the behavior of the pressure and of the deformation at the edge of the domain always has the form $p = f\sqrt{|\Delta x|}$ and $h = 4f(1 - \sigma^2)|\Delta x|^{3/2}/(3E)$ of the two-dimensional problem (Δx is the distance from the edge, and f is a constant), as a local analysis reveals.⁹ This means the boundary conditions on the similarity solution for $\xi \rightarrow \pm\infty$ carry over as well. Thus the above local solution of (12) can be applied unchanged, except for an effective radius R which enters, and whose value might have to be determined from a numerical solution of the contact problem.

In the case of a three-dimensional body, supporting a force F (rather than a force per unit length L), the edge of the contact area is a closed curve in the plane, see Fig. 3 for the example of a sphere. In the limit of small λ , the boundary layer is much thinner than the radius of curvature of the edge, and gradients are dominated by the derivative in the direction of the normal vector. This means that U is replaced by $U \cos\theta$, where θ is the angle between the normal and the direction of motion, but otherwise the similarity equations remain the same. A problem, however, does exist for the neighborhood of $\theta = \pi/2$, for which the normal speed vanishes, and for which a special asymptotic region needs to be found. Using the contact radius $a = (3FR(1 - \sigma^2)/4E)^{1/3}$ and $h_{3D} = 4a^2/(\pi R)$ to non-dimensionalize the radial variable r and the film thickness, respectively, the Hertz solution for the sphere⁸ leads to the identification

$$\lambda_{3D} = \frac{\pi^3}{48^{1/3}} \frac{\eta U \cos\theta R^{5/3} E^{1/3}}{F^{4/3} (1 - \sigma^2)^{1/3}} \quad (14)$$

with $f = \sqrt{2}$, as in the cylindrical case. As seen in Fig. 3 (top), this provides excellent agreement with the similarity profile calculated earlier, for various angles along the inlet side of the contact. To connect to the outlet, one needs to solve the hyperbolic equation

$$\nabla(\nabla p h^3) = \frac{\lambda_{3D}}{\cos\theta} h_x \quad (15)$$

for the film thickness, valid in the interior of the contact.³¹ One can show that for $\lambda_{3D} \rightarrow 0$ the characteristics of (15) are parallel to \mathbf{U} , so the constant H^* for the outlet is determined by the corresponding inlet solution under the same angle θ .

In conclusion, our similarity theory predicts film profiles which agree well with numerical simulations, and the scaling of the film thickness is confirmed by experiment. In many engineering applications, such as joints or bearings, pressures are large, so that the fluid viscosity becomes pressure-dependent.⁴ However, the structure of the solution is still very similar to the profiles we find. An asymptotic analysis of the case of large viscosity variations still needs to be performed. Our theory also provides a physical rationale for an important empirical finding based on the results of many numerical solutions of 2D and 3D problems with surface waviness: the deformation of surface patterns in highly loaded contacts is uniquely determined by the ratio of the wavelength of the perturbation to a so-called “inlet length.”³² This “inlet length” can now be understood as the scale of the boundary layer identified in this Letter.

- ¹ B. J. Hamrock, S. R. Schmid, and B. O. Jacobson, *Fundamentals of Fluid Film Lubrication*, 2nd ed. (Marcel Dekker, New York, 2004).
- ² J. M. Skotheim and L. Mahadevan, “Soft lubrication,” *Phys. Rev. Lett.* **92**, 245509 (2004).
- ³ J. M. Skotheim and L. Mahadevan, “Soft lubrication: The elastohydrodynamic of nonconforming and conforming contacts,” *Phys. Fluids* **17**, 092101 (2005).
- ⁴ R. Gohar and H. Rahnejat, *Fundamentals of Tribology* (Imperial College Press, London, 2012).
- ⁵ R. Gohar, *Elastohydrodynamics*, Ellis Horwood Series in Engineering Science (E. Horwood, Chichester, West Sussex, 1988).
- ⁶ C. H. Venner and A. A. Lubrecht, *Multilevel Methods in Lubrication* (Elsevier, Amsterdam, 2000).
- ⁷ J. Urzay, S. G. Llewellyn Smith, and B. J. Glover, “The elastohydrodynamic force on a sphere near a soft wall,” *Phys. Fluids* **19**, 103106 (2007).
- ⁸ L. D. Landau and E. M. Lifshitz, *Elasticity* (Pergamon, Oxford, 1984).
- ⁹ C. J. Hooke and J. P. O’Donoghue, “Elastohydrodynamic lubrication of soft, highly deformed contacts,” *J. Mech. Eng. Sci.* **14**, 34 (1972).
- ¹⁰ E. J. Bissett, “The line contact problem of elastohydrodynamic lubrication. I. Asymptotic structure for low speeds,” *Proc. R. Soc. London, Ser. A* **424**, 393 (1989).
- ¹¹ E. J. Bissett and D. A. Spence, “The line contact problem of elastohydrodynamic lubrication. II. Numerical solutions of the integrodifferential equations in the transition exit layers,” *Proc. R. Soc. London, Ser. A* **424**, 409 (1989).
- ¹² J. Eggers and M. A. Fontelos, “The role of self-similarity in singularities of partial differential equations,” *Nonlinearity* **22**, R1 (2009).
- ¹³ F. P. Bretherton, “The motion of long bubbles in tubes,” *J. Fluid Mech.* **10**, 166 (1961).
- ¹⁴ G. K. Batchelor, *An Introduction to Fluid Dynamics* (Cambridge University Press, Cambridge, 1967).
- ¹⁵ D. Dowson and G. R. Higginson, *Elastohydrodynamic Lubrication, the Fundamentals of Roller and Gear Lubrication* (Pergamon Press, Oxford, UK, 1966).
- ¹⁶ P. M. Lugt, *Grease Lubrication in Rolling Bearings* (Wiley, 2013).
- ¹⁷ R. H. Davis, J.-M. Serayssol, and E. J. Hinch, “The elastohydrodynamic collision of two spheres,” *J. Fluid Mech.* **163**, 479 (1986).
- ¹⁸ J. Ashmore, C. del Pino, and T. Mullin, “Cavitation in a lubrication flow between a moving sphere and a boundary,” *Phys. Rev. Lett.* **94**, 124501 (2005).
- ¹⁹ K. L. Johnson, *Contact Mechanics* (Cambridge University Press, 1985).
- ²⁰ H. Hochstadt, *Integral Equations* (John Wiley, 1973).
- ²¹ K. Herrebrugh, “Solving the incompressible and isothermal problem in elastohydrodynamic lubrication through an integral equation,” *ASME J. Lubr. Technol.* **90**, 262 (1968).
- ²² W. H. Press, S. A. Teukolski, W. T. Vetterling, and B. P. Flannery, *Numerical Recipes* (Cambridge University Press, Cambridge, 1992).
- ²³ J. Seiwert, D. Quéré, and C. Clanet, “Flexible scraping of viscous fluids,” *J. Fluid Mech.* **715**, 424 (2013).
- ²⁴ A. Brandt and A. A. Lubrecht, “Multilevel matrix multiplication and the fast solution of integral equations,” *J. Comput. Phys.* **90**, 348–370 (1990).
- ²⁵ R. Gohar and A. Cameron, “Optical measurement of oil film thickness under elasto-hydrodynamic lubrication,” *Nature (London)* **200**, 458 (1963).
- ²⁶ A. D. Roberts and P. D. Swales, “The elastohydrodynamic lubrication of a highly elastic cylindrical surface,” *J. Phys. D* **2**, 1317 (1969).
- ²⁷ A. Martin, J. Clain, A. Buguin, and F. Brochard-Wyart, “Wetting transitions of soft, sliding interfaces,” *Phys. Rev. E* **65**, 031605 (2002).
- ²⁸ P.-G. de Gennes, F. Brochart-Wyart, and D. Quéré, *Capillarity and Wetting Phenomena: Drops, Bubbles, Pearls, Waves* (Springer, 2003).
- ²⁹ S. P. Meeker, R. T. Bonnecaze, and M. Cloitre, “Slip and flow of soft particle pastes,” *Phys. Rev. Lett.* **92**, 198302 (2004).
- ³⁰ S. P. Meeker, R. T. Bonnecaze, and M. Cloitre, “Slip and flow in pastes of soft particles: Direct observation and rheology,” *J. Rheol.* **48**, 1295 (2004).
- ³¹ C. J. Hooke, “Calculation of clearances in soft point contacts,” *J. Tribol.* **110**, 167 (1988).
- ³² C. J. Hooke and C. H. Venner, “Surface roughness attenuation in line and point contacts,” *J. Eng. Tribol.* **214**, 439 (2000).